frontiers in Cellular Neuroscience

ORIGINAL RESEARCH
published: 03 May 2019
doi: 10.3389/fncel.2019.00125

A Tripartite Interaction Among the Calcium Channel α_1- and β-Subunits and F-Actin Increases the Readily Releasable Pool of Vesicles and Its Recovery After Depletion

Gustavo A. Guzman[1], *Raul E. Guzman*[1], *Nadine Jordan*[1] *and Patricia Hidalgo*[1,2]*

[1]*Institute of Complex Systems 4, Zelluläre Biophysik, Forschungszentrum Jülich, Jülich, Germany,* [2]*Institute of Biochemistry, Heinrich-Heine University, Düsseldorf, Germany*

Neurotransmitter release is initiated by the influx of Ca^{2+} *via* voltage-gated calcium channels. The accessory β-subunit ($Ca_V\beta$) of these channels shapes synaptic transmission by associating with the pore-forming subunit ($Ca_V\alpha_1$) and up-regulating presynaptic calcium currents. Besides $Ca_V\alpha_1$, $Ca_V\beta$ interacts with several partners including actin filaments (F-actin). These filaments are known to associate with synaptic vesicles (SVs) at the presynaptic terminals and support their translocation within different pools, but the role of $Ca_V\beta$/F-actin association on synaptic transmission has not yet been explored. We here study how $Ca_V\beta_4$, the major calcium channel β isoform in mamalian brain, modifies synaptic transmission in concert with F-actin in cultured hippocampal neurons. We analyzed the effect of exogenous $Ca_V\beta_4$ before and after pharmacological disruption of the actin cytoskeleton and dissected calcium channel-dependent and -independent functions by comparing the effects of the wild-type subunit with the one bearing a double mutation that impairs binding to $Ca_V\alpha_1$. We found that exogenously expressed wild-type $Ca_V\beta_4$ enhances spontaneous and depolarization-evoked excitatory postsynaptic currents (EPSCs) without altering synaptogenesis. $Ca_V\beta_4$ increases the size of the readily releasable pool (RRP) of SVs at resting conditions and accelerates their recovery after depletion. The enhanced neurotransmitter release induced by $Ca_V\beta_4$ is abolished upon disruption of the actin cytoskeleton. The $Ca_V\alpha_1$ association-deficient $Ca_V\beta_4$ mutant associates with actin filaments, but neither alters postsynaptic responses nor the time course of the RRP recovery. Furthermore, this mutant protein preserves the ability to increase the RRP size. These results indicate that the interplay between $Ca_V\beta_4$ and F-actin also support the recruitment of SVs to the RRP in a $Ca_V\alpha_1$-independent manner. Our studies show an emerging role of $Ca_V\beta$ in determining SV maturation toward the priming state and its replenishment after release. We envision that this subunit plays a role in coupling exocytosis to endocytosis during the vesicle cycle.

Keywords: calcium channel, $Ca_V\beta$ subunits, F-actin, RRP size, RRP refilling, EPSC

OPEN ACCESS

Edited by:
Alfredo Kirkwood, Johns Hopkins University, United States

Reviewed by:
Fernando Diego Marengo, IFIBYNE (UBA—CONICET), Argentina
Diasynou Fioravante, University of California, Davis, United States

***Correspondence:**
Patricia Hidalgo
pa.hidalgo@fz-juelich.de

Received: *13 November 2018*
Accepted: *13 March 2019*
Published: *03 May 2019*

Citation:
Guzman GA, Guzman RE, Jordan N and Hidalgo P (2019) A Tripartite Interaction Among the Calcium Channel α_1- and β-Subunits and F-Actin Increases the Readily Releasable Pool of Vesicles and Its Recovery After Depletion. Front. Cell. Neurosci. 13:125. doi: 10.3389/fncel.2019.00125

INTRODUCTION

Calcium entry through $Ca_V2.x$ high-voltage activated calcium channels is a pivotal step during action potential-evoked neurotransmitter release and synaptic plasticity (Wheeler et al., 1994; Cao and Tsien, 2010; Simms and Zamponi, 2014; Nanou and Catterall, 2018). The $Ca_V2.x$ calcium channel core complex in the mammalian brain is composed of one $Ca_V\alpha_1$ and one $Ca_V\beta$ subunit (Müller et al., 2010).

The $Ca_V\beta$ family belongs to the membrane-associated guanylate kinases (MAGUKs) class of scaffolding proteins encompassing two highly conserved domains, a Src 3 homology (SH3) domain and a guanylate kinase (GK) domain that are flanked by variable regions (Chen et al., 2004; Opatowsky et al., 2004; Van Petegem et al., 2004). The four $Ca_V\beta$ isoforms described until now, $Ca_V\beta_1$ to $Ca_V\beta_4$, associate with a highly conserved sequence among the high-voltage activated $Ca_V\alpha_1$ referred to as α_1 interaction domain (AID) that is located within the intracellular loop joining the transmembrane domains I and II (Pragnell et al., 1994). Association of $Ca_V\beta$ with the AID site increases calcium current densities by altering the biophysical properties of the channel and its expression at the plasma membrane (Buraei and Yang, 2010). Accordingly, in mouse hippocampal neurons exogenously expressed $Ca_V\beta_4$, the predominant $Ca_V\beta$ isoform associated with the $Ca_V2.x$ core complex (Müller et al., 2010), increases neurotransmitter release *via* slowing down voltage-dependent inactivation and promoting $Ca_V2.x$ channel cell surface expression (Wittemann et al., 2000; Xie et al., 2007; Etemad et al., 2014).

Several lines of evidence suggest that $Ca_V\beta_4$ affects synaptic transmission by mechanisms that are independent of the upregulation of $Ca_V2.x$-mediated currents. Dissociation from $Ca_V\alpha_1$ induced by membrane depolarization favors the association of $Ca_V\beta_{4b}$ with a phosphatase 2A regulatory subunit causing their translocation to the nucleus and regulation of transcriptional activity (Tadmouri et al., 2012; Ronjat et al., 2013). $Ca_V\beta_{4b}$ also associates with the Rab3 interacting molecule RIM1 and facilitates synaptic transmission by supporting the docking of synaptic vesicles (SVs; Kiyonaka et al., 2007).

We have previously shown that the $Ca_V\beta_2$ isoform associates directly with F-actin and facilitates the trafficking of $Ca_V\alpha_1$-containing transport vesicles toward the plasma membrane (Stölting et al., 2015; Conrad et al., 2018). The actin-based cytoskeleton supports readily releasable pool (RRP) recruitment, docking step and recycling of SVs as well as of synaptic proteins after neurotransmitter release (Cingolani and Goda, 2008; Hallermann and Silver, 2013; Tanifuji et al., 2013; Hayashida et al., 2015; Rust and Maritzen, 2015; Miki et al., 2016). These two lines of evidence motivated us to investigate whether the interaction between $Ca_V\beta$ and the actin cytoskeleton play a role in the recruitment of SVs to the active zone and replenishment after depletion. In order to dissect $Ca_V\alpha_1$-dependent and independent functions (Hidalgo and Neely, 2007; Hofmann et al., 2015; Rima et al., 2016), we generated a wild-type (WT) $Ca_V\beta_{4b}$ and a mutant version with disrupted binding to $Ca_V\alpha_1$ (Opatowsky et al., 2004) and, expressed these constructs in primary mouse hippocampal neurons.

We found that $Ca_V\beta_{4b}$ also binds to actin filaments (F-actin) and, at excitatory synapses it enhances spontaneous and evoked postsynaptic currents as well as the size of the RRP of SVs and its recovery time after depletion. The enhanced synaptic transmission relies on the association of $Ca_V\beta_{4b}$ with $Ca_V\alpha_1$ and depends on an intact actin cytoskeleton. $Ca_V\beta_{4b}$ mutant retains the capability to interact with F-actin and to recruit SVs to the RRP, but it fails to increase neurotransmitter release. Our results add a new function of $Ca_V\beta_4$ in shaping synaptic transmission and expand the already broad functional repertoire of this subunit.

MATERIALS AND METHODS

cDNA Constructs

For heterologous expression of $Ca_V2.2/Ca_V\beta_{4b}$ in HEK293T cells, the cDNA-encoding region of the human $Ca_V2.2\alpha_1$ pore-forming subunit of voltage-gated calcium channels (UniProtKB: Q00975-1) was subcloned into pEGFP-N1 to yield a C-terminal $Ca_V2.2$-GFP fusion protein. The human WT $Ca_V\beta_{4b}$ (UniProtKB: O00305.2) was fused to mCherry to facilitate recognition of transfected cells. For recordings in hippocampal neurons, cDNA-encoding WT and $Ca_V\alpha_1$-association deficient $Ca_V\beta_{4b}$ mutant where fused to eGFP and subcloned into FsY1.1 G.W lentiviral transfer vector (kindly provided by Dr. M Filippov, Nizhny Novgorod, Russia) to yield fusion constructs with the eGFP moiety fused at the C-terminus of $Ca_V\beta_{4b}$. To express a $Ca_V\beta_{4b}$ mutant with impaired $Ca_V\alpha_1$-association M238A/L384A amino acid substitutions were introduced by PCR based techniques. For protein expression in *E.coli*, the coding region of the core regions of $Ca_V\beta_{4b}$ (residues 50–408) or $Ca_V\beta_{2a}$ (UniProtKB: Q8VGC3-2) was subcloned into pRSETB vector (Invitrogen, Carlsbad, CA, USA) as described (Stölting et al., 2015). All constructs were verified by DNA sequencing.

Recombinant Proteins

Histidine-tagged $Ca_V\beta$ derivatives were purified from *E.coli* lysates as previously described (Hidalgo et al., 2006). In brief, proteins were purified from the soluble fraction of the crude lysate by metal affinity followed by size-exclusion chromatography. Fractions containing the purified proteins were concentrated and stored at −80°C until use. The glutathione S-transferase (GST) protein alone or fused to the $Ca_V\alpha_1$-anchoring domain (AID) have been previously described (Miranda-Laferte et al., 2014). The GST pull-down assay was done as previously (Hidalgo et al., 2006) and also described in **Supplementary Material**.

F-Actin Cosedimentation Assay

Binding of the $Ca_V\beta$ derivatives to F-actin was studied using the F-actin co-sedimentation assay according to the manufacturer's instructions (Cytoskeleton, Inc, Denver, CO, USA) and as previously described (Stölting et al., 2015). Each assay was performed in a volume of 50 µl. For each reaction, either protein alone (control) or together with F-actin, the same amount and stock of $Ca_v\beta$ was used. Briefly, the purified proteins were

incubated with rabbit muscle actin in actin polymerization buffer containing (in mM): 10 Tris-HCl, 0.2 $CaCl_2$, 50 KCl, 2 $MgCl_2$, 1 ATP, pH 8.0, centrifuged for 1 h at 150,000× *g* at 4°C in a Beckman TLA 100.1 rotor. After centrifugation, the whole supernatant was transferred to a new tube while the pellet was resuspended in a final volume of 50 µl containing 1× SDS-loading buffer. Supernatant and pellet fractions were then resolved by denaturing SDS-PAGE. Each lane was loaded with 25 µl to permit direct comparison of protein amounts bound or unbound to F-actin. Since $Ca_V\beta_{4b}$ core and actin exhibit overlapping migration in the mini gels (Bio-Rad, Hercules, CA, USA), the proteins were resolved using a Multigel-Long chamber (Biometra, Göttingen, Germany). Proteins were visualized with Coomassie Blue and the prestained protein markers Dual color (Bio-Rad, Hercules, CA, USA) or PageRuler Plus (Thermo Fisher, Waltham, MA, USA) were used as molecular mass standards. All assays were repeated at least three times.

Cell Culture and Immunocytochemistry

Autaptic and mass cultures of hippocampal neurons were prepared from postnatal day 0 to day 3 C57/BL6-N mice and maintained as previously described (Guzman et al., 2010). Briefly, hippocampi were isolated from brain and enzymatically treated with 15 units of papain (Worthington Biochemical Corp, Lakewood, NJ, USA) for 20 min at 37°C. After enzymatic digestion, neurons were mechanically dissociated. For autaptic cultures, neurons were diluted to a density of 1,000 cells/ml and plated onto micro-islands containing glial cells that were cultured 3–5 days prior to seeding neurons. For mass cultures, isolated neurons were diluted to a density of 300 cells/cm^2 on 25 mm glass coverslips previously treated with poly-D-lysine (Sigma-Aldrich, St. Louis, MO, USA). Neuronal cells were grown in NBA (Invitrogen, Carlsbad, CA, USA), supplemented with Glutamax at 1% (Thermo Fisher, Waltham, MA, USA) penicillin/streptomycin at 2% (Thermo Fisher, Waltham, MA, USA) and B-27 at 2% (Thermo Fisher, Waltham, MA, USA). Neurons were used after 10–14 days *in vitro* (DIV) for electrophysiological recordings and for fluorescence confocal microscopy imaging. HEK293T cells (Sigma-Aldrich, St. Louis, MO, USA) used for electrophysiological recordings of heterologously expressed $Ca_V2.2$ were cultivated in cell culture dishes using DMEM (Gibco) medium supplemented with 10% FBS and with 2% penicillin/streptomycin. All cells were cultivated at 37°C and in a humidified atmosphere with 5% CO_2.

Virus Production, Transduction of Hippocampal Neurons and HEK Cells Transfection

To deliver the cDNA encoding for the $Ca_V\beta_{4b}$ constructs hippocampal cultures were infected with lentivirus. The helper plasmids pRSVREV, pMDLg/pRRE, and vesicular stomatitis virus G protein expressing plasmid were kindly provided by Dr. Thomas Südhof (Howard Hughes Medical Institute, Stanford University, Stanford, CA, USA). Lentivirus was produced (Barde et al., 2010) and transduced as previously described (Stölting et al., 2015). Calcium phosphate transfection was used to co-transfect the lentiviral transfer vector and the three helper plasmids into HEK293FT cells. After 14 h transfection, cell culture medium containing (DMEM, 10% FBS, 100 mM sodium pyruvate, 100 mM non-essential amino acids, and 100 mM Glutamax) was renewed. Solutions were purchased from Thermo Fisher (Waltham, MA, USA). Cell culture medium containing lentiviral particles was withdrawn from the cell surface and ultracentrifuged for 2 h. Lentiviral particles were immediately resuspended in culture medium, frozen in liquid nitrogen and stored at −80°C. Hippocampal neurons were infected using 30–50 µl of viral suspension at 1–3 DIV.

HEK cells were transiently co-transfected with $Ca_V2.2$-GFP and either with WT or mutant $Ca_V\beta_{4b}$-mCherry using Lipofectamine 2000™ (Invitrogen, Carlsbad, CA, USA). Cells were split 12 h after transfection, and the electrophysiological experiments were performed 24 h later.

Immunostaining and Confocal Microscopy

Mass hippocampal neurons infected with lentiviral particles encompassing the $Ca_V\beta_{4b}$-eGFP constructs were fixed with 4% paraformaldehyde (PFA) in PBS during 10 min at room temperature (RT). PFA was removed and 0.1% Triton X-100 in PBS was added to neurons and incubated at RT for 10 min. Primary antibodies incubation using anti-MAP-2 (Synaptic Systems, Göttingen, Germany), and anti-VGLUT1 (Synaptic Systems, Göttingen, Germany) was performed overnight at 4°C. Transduced neurons were incubated with anti-GFP (Abcam, Cambridge, UK) to enhance eGFP fluorescence. Samples were then rinsed five times with PBS and incubated with secondary antibodies conjugated either with 647-Alexa (Thermo Fisher, Waltham, MA, USA), Dylight 549 (Jackson ImmunoResearch, UK) or 488-Alexa (Thermo Fisher, Waltham, MA, USA) for 60 min at RT. After washing in PBS three times, samples were fixed in mounting medium and confocal images were acquired with a Leica TCS SP5 II inverted microscope (Leica Microsystems, Wetzlar, Germany) equipped with a ×63 oil immersion objective. Alexa fluorophores, 488 and 647, were excited with a 488-nm argon laser and with a 633-nm helium-neo laser, respectively. Emission signals were acquired after filtering with 500–550 nm and 640–700 nm bandpass filters, respectively. Dylight 549 was excited with a 543-nm helium-neo laser and emission signal was acquired after filtering with 570–610 nm bandpass filter. Changes in synapse formation were evaluated by analyzing the synaptic contact density per 50 µm length of neuronal structures. Overlapping positive puncta structures were identified between immunolabeled signals generated by presynaptic and postsynaptic markers. Confocal images were analyzed using Fiji ImageJ (Schindelin et al., 2012).

Electrophysiology

Electrophysiological studies were conducted using the whole-cell voltage-clamp configuration with an EPC-10 amplifier equipped with the PatchMaster software (HEKA, Elektronik). Excitatory postsynaptic currents (EPSCs) were obtained from autaptic neuronal cultures containing a layer of glial cells and a single neuron forming autapses as described (Guzman et al., 2010). The composition of the external recording solution was (in

mM): 130 NaCl, 10 $NaHCO_3$, 2.4 KCl, 1.25 $CaCl_2$, 1.3 $MgCl_2$, 10 HEPES, 10 D-glucose, pH 7.3 with NaOH, osmolarity, 310 mOsm. The extracellular solution was supplemented with 20 μM bicuculline (Tocris Bioscience, Bristol, UK) to ensure the recording of EPSCs. Borosilicate patch pipettes with resistances of 3.5–6 MΩ were pulled on a Sutter P-1000 puller (Sutter, Novato, CA, USA) and filled with the intracellular solution containing (in mM): 137.5 K-gluconate, 11 NaCl, 4 MgATP, 0.4 Na_2GTP, 1.1 EGTA, 11 HEPES, 11 D-glucose, pH 7.3 with CsOH, osmolarity, 310 mOsm. EPSCs were triggered by a brief somatic depolarization from a holding potential of −70 mV to +10 mV during 0.7 ms. Data were registered at 10 or 50 kHz and Bessel filtered at 3.0 kHz. The resulting series resistance was usually less than 12 MΩ, and only neurons with series resistance below 15 MΩ and 70% to 85% resistance compensation were used for analysis. The amplitude of the evoked current was calculated from the baseline amplitude subtracted prior to stimulation artifact. The amount of the RRP of vesicles was measured by application of a hypertonic sucrose solution (500 mM) for 4 s with aid of a fast-flow perfusion system (AutoMate Scientific, Berkeley, CA, USA). The amplitude and charge of evoked EPSCs and the charge of RRP sucrose responses were evaluated by means of the following software: Clampfit (Molecular Devices, San Jose, CA, USA) and OriginPro (OriginLab Corporation, Northampton, MA, USA). The RRP size has been estimated as previously described (Stevens and Sullivan, 1998). The replenishment of RRP was measured after RRP depletion by applying paired-pulses of hypertonic sucrose solution during 3 s at 1 s, 3 s, 7 s, 15 s, 30 s and 60 s. Then, the time course of RRP refilling was analyzed by calculating firstly the percentage of RRP recovery at several interpulse time intervals relative to the last application of hypertonic sucrose (60 s). Second, the percentage of RRP recovery was fitted to a single exponential function to simplify the analysis of data as proposed (Stevens and Wesseling, 1998). To evaluate postsynaptic receptor saturation, 1 mM γ–D-Glutamylglycine (Tocris Bioscience, Bristol, UK) was added to the sucrose solution as described in **Supplementary Figure S6**. Miniature excitatory spontaneous postsynaptic currents (mEPSCs) were recorded in mass hippocampal neurons at holding potential of −70 mV during 1 min in the presence of 20 μM bicucullin and 1 μM tetrodotoxin (TTX; Biotrend, Köln, Germany) which was added to the standard extracellular solution to avoid spontaneous depolarization of the neurons. Spontaneous events with peak amplitudes higher than 15 pA (∼5 times the standard deviation of the background noise) and with charges higher than 25 fC were evaluated using the software MiniAnalysis by Synaptosoft. Data were sampled at 10 kHz and Bessel filtered at 3.0 kHz. Recordings of $Ca_V2.2/Ca_V\beta_{4b}$-mediated currents in HEK293T cells are described in **Supplementary Material**.

Statistical Analysis

The data are presented as column scatter dot plots with the mean value ± standard error of the mean (SEM) of each distribution shown by a line. Experiments were conducted in at least three different cell culture preparations with at least three different batches of lentivirus. Statistical significance was analyzed by a comparison between the data sets using one-way analysis of variance (ANOVA). p values: $^{*}p < 0.05$, $^{**}p < 0.01$, $^{***}p < 0.001$ were considered statistically significant. The variability between tested groups was conducted with SigmaPlot version 12.3 (Systat Software, San Jose, CA, USA). The data obtained to calculate the time course of replenishment of RRP were fitted with OriginPro.

RESULTS

$Ca_V\beta$ Associates With Actin Filaments and the $Ca_V\alpha_1$-Anchoring Domain in a Non-exclusive Manner

We used an *in vitro* co-sedimentation assay to test the association of $Ca_V\beta_{4b}$ with actin filaments. For this assay, actin is dissolved in a low salt polymerization buffer to promote the formation of F-actin. After centrifugation, proteins that associate with F-actin are recovered from the pellet fraction. Since recombinant full-length $Ca_V\beta_s$ are not stable under low salt conditions (Stölting et al., 2015), we purified the core of the human neuronal $Ca_V\beta_{4b}$ containing the two highly conserved SH3 and GK domains. We verified that $Ca_V\beta_{4b}$ core associates with F-actin as previously described for the core domain derived from $Ca_V\beta_2$ (Stölting et al., 2015; **Figures 1A,B** and **Supplementary Figure S1**).

We next examined if the interaction of $Ca_V\beta$ with F-actin and $Ca_V\alpha_1$ are mutually exclusive or not. To assess $Ca_V\beta$-$Ca_V\alpha_1$ association, the highly conserved AID site (Pragnell et al., 1994) was fused to GST (GST-AID) as previously described (Hidalgo et al., 2006). The $Ca_V\beta_{4b}$ protein construct bearing a double mutation at two residues critical for association with the AID domain (M238A/L384A, **Figure 1A**; Chen et al., 2004; Opatowsky et al., 2004) resulted in low yield and poor stability in low salt buffers. Thus, we used the core of $Ca_V\beta_2$ as background and introduced the two point mutations at the analogous residues. This $Ca_V\alpha_1$ association-deficient $Ca_V\beta_2$ core mutant is more stable in the F-actin polymerization buffer and preserves the ability to associate with F-actin (**Figure 1C**). GST-AID co-sedimented together with F-actin in the presence of WT $Ca_V\beta_2$, but not of the mutant version with impaired AID association (**Figure 1D**).

These results demonstrate that GST-AID is mobilized to the pellet fraction, together with F-actin, through its association with $Ca_V\beta$. We conclude that $Ca_V\beta$ can simultaneously associate with $Ca_V\alpha_1$ and F-actin.

$Ca_V\beta_{4b}$ Increases the Frequency of Miniature Excitatory Postsynaptic Currents in the Presence of an Intact Actin Cytoskeleton

To study the functional role of the $Ca_V\beta_{4b}$/F-actin association in synaptic transmission, we generated two lentiviral gene delivery expression vectors encoding either full-length $Ca_V\beta_{4b}$ (hereafter denoted as $\beta_{4\text{-WT}}$) or the $Ca_V\beta_{4b}$ M238A/L384A mutant with

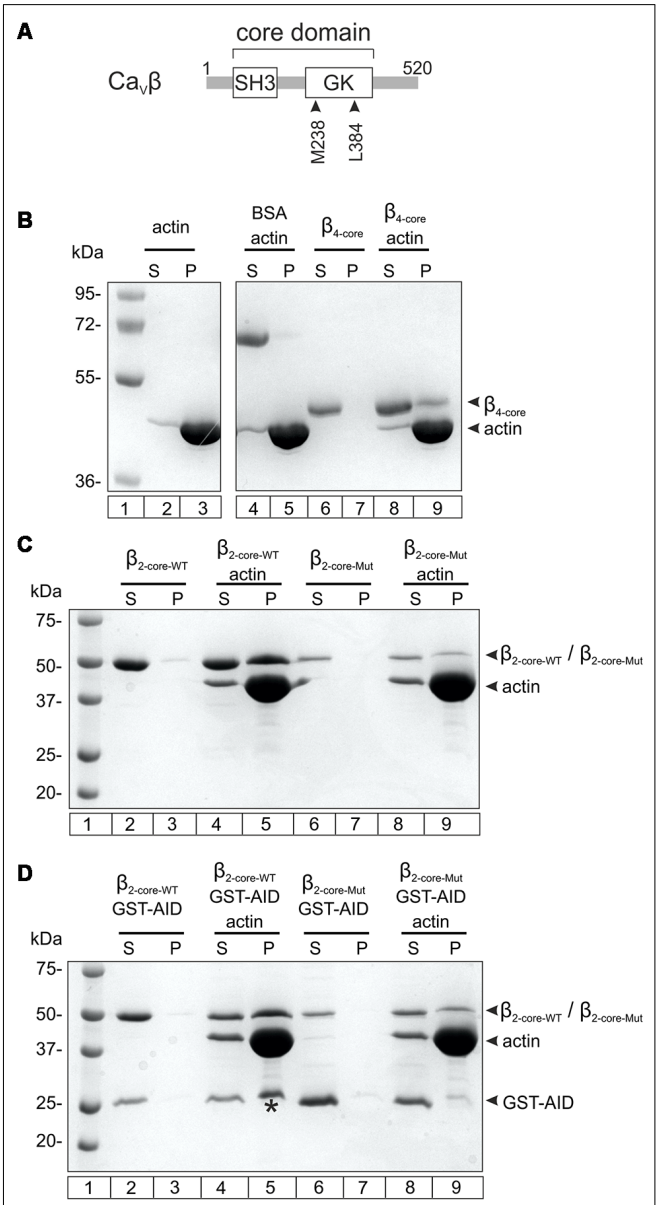

FIGURE 1 | Nonexclusive association between $Ca_v\beta$ with the $Ca_v\alpha_1$ anchoring domain and with F-actin. **(A)** Scheme showing the two-domain architecture of $Ca_V\beta$. The numbers correspond to the amino acid position of the $Ca_V\beta_{4b}$ sequence used in this study. SH3, Src homology domain, GK, guanylate kinase domain. **(B)** F-actin cosedimentation assay examining the association of $Ca_V\beta_{4b}$ core (residues 50–408, $\beta_{4\text{-core}}$) with actin filaments. After incubating actin alone in the polymerization buffer or together with $\beta_{4\text{-core}}$, the proteins were centrifuged and the supernatant (S) and pellet (P) fractions separated and resolved by SDS-denaturing PAGE. The numbers denote the mass in kDa of standard molecular markers (lane 1). The vast majority of actin polymerizes and pelleted after centrifugation (lanes 2–3). BSA, used as negative control, does not co-sediment with F-actin (lanes 4–5). $\beta_{4\text{-core}}$ alone is found in the supernatant after centrifugation (lanes 6–7) and in the pellet fraction when incubated with F-actin (lanes 8–9). For clarity, irrelevant lanes were cropped from the source image (indicated by the white space) and the full image is shown in the **Supplementary Figure S1**. **(C)** F-actin cosedimentation assay using the wild-type $Ca_V\beta_2$ core region ($\beta_{2\text{-core-WT}}$) and a mutant with impaired association with the AID site (*Continued*)

FIGURE 1 | Continued
($\beta_{2\text{-core-Mut}}$). $\beta_{2\text{-core-WT}}$ alone and $\beta_{2\text{-core-Mut}}$ alone are recovered from the supernatant fraction after centrifugation (lanes 2–3 and 6–7, respectively) and in the presence of F-actin they are found in the pellet (lanes 4–5 and 8–9, respectively). **(D)** F-actin cosedimentation assay as in **(C)**, but in the presence of glutathione S-transferase (GST) fused to the AID site (GST-AID). In the absence of F-actin, GST-AID with either $\beta_{2-core\text{-}WT}$ or $\beta_{2\text{-core-Mut}}$ is all found in the supernatant fraction after centrifugation (lanes 2–3 and 6–7, respectively). In the presence of F-actin, GST-AID is recovered in the pellet (denoted by an asterisk) only with $\beta_{2-core\text{-}WT}$ (lanes 4–5), but not with the mutant subunit (lanes 8–9). All assays were repeated at least three times.

impaired $Ca_V\alpha_1$-binding (hereafter denoted as $\beta_{4\text{-Mut}}$). Both $Ca_V\beta_{4b}$ constructs were linked to either eGFP or mCherry at their carboxy-terminal ends for visualization by fluorescence microscopy. $\beta_{4\text{-WT}}$, but not β_{4-Mut}, expressed in HEK293T associated *in vitro* with GST-AID (**Supplementary Figure S2A**) and when expressed together with $Ca_V2.2$ supported robust ionic currents (**Supplementary Figures S2B,C**). $\beta_{4\text{-Mut}}$ failed to yield $Ca_V2.2$-mediated currents.

In mass cultures of dissociated hippocampal neurons exogenous $\beta_{4\text{-WT}}$ and $\beta_{4\text{-Mut}}$ accumulate in synapses as judged by the co-localization with the presynaptic and postsynaptic markers VGLUT-1 and the MAP2, respectively (**Figures 2A,B**). We analyzed the number of excitatory synaptic contacts (VGLUT-1 positives puncta) in non-transfected hippocampal neurons and neurons expressing either $\beta_{4\text{-WT}}$ or β_{4-Mut} by immunostaining (**Figures 2A–C**). Neither $\beta_{4\text{-WT}}$ nor β_{4-Mut} alters synapse density at excitatory synapses (**Figure 2D**). Thus, exogenous $Ca_V\beta_{4b}$ does not modify synaptogenesis.

We recorded mEPSCs in mass cultures of hippocampal neurons transduced with the $Ca_V\beta_{4b}$-encoding plasmids (**Figure 3**). We found that $\beta_{4\text{-WT}}$ significantly increased the average frequency of the mEPSCs, whereas $\beta_{4\text{-Mut}}$ produced no changes (**Figures 3A,B**). No alterations in the mean decay time constant of the averaged mEPSC responses were observed in neurons expressing $\beta_{4\text{-WT}}$ or $\beta_{4\text{-Mut}}$ with respect to non-transduced cells (**Figure 3C**). The increased mEPSC frequency combined with the absence of alterations in mEPSCs decay time and in synapse density suggests a presynaptic function of $Ca_V\beta_{4b}$ in modulating neurotransmitter release as proposed (Wittemann et al., 2000; Xie et al., 2007). Both $Ca_V\beta_{4b}$ constructs induced a reduction in the average amplitude and charge transfer of the mEPSCs (**Figures 3D,E**), resulting in a slight leftward shift of the corresponding cumulative probability curve of the mEPCS with respect to the distribution obtained from non-transduced neurons (**Supplementary Figures S3A,B**). These changes may arise from a decreased vesicular loading or from a reduction in the density of functional postsynaptic receptors triggered by $Ca_V\beta_4$. Up-to-date there is no evidence associating $Ca_V\beta_4$ with SV glutamate loading (Blondeau et al., 2004; Morciano et al., 2005; Takamori et al., 2006). Furthermore, since $Ca_V\beta_4$ can be also targeted postsynaptically (Wittemann et al., 2000; Xie et al., 2007), we favor the idea that postsynaptic mechanisms account for these rather minor differences.

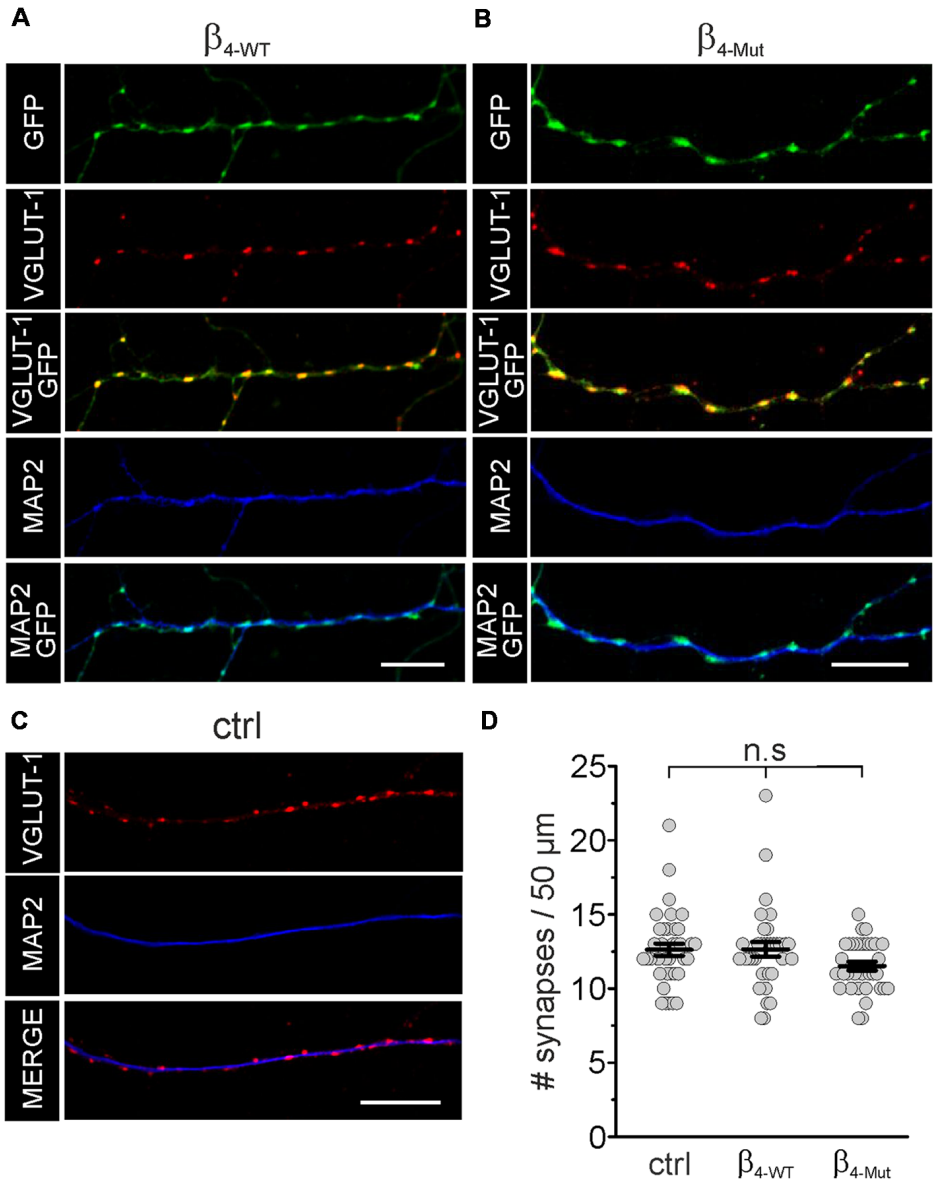

FIGURE 2 | Exogenous WT $Ca_V\beta_{4b}$ and the $Ca_v\alpha_1$ association-deficient mutant are targeted to synaptic contacts and do not alter synapse density in hippocampal neurons. Laser scanning confocal images of hippocampal neurons either transduced with $Ca_V\beta_{4b}$ WT ($\beta_{4\text{-WT}}$) fused to eGFP **(A)** or with $Ca_V\beta_{4b}$ mutant with impaired $Ca_V\alpha_1$ binding ($\beta_{4\text{–}Mut}$) fused to eGFP **(B)** and non-transduced neurons (ctrl; **C**). Neurons were immunolabeled with the glutamatergic presynaptic terminal marker VGLUT-1 (red) and the dendrite-selective marker MAP2 (blue). $Ca_V\beta_{4b}$ fluorescence signal is shown in green. **(D)** Scatter dot plot of the number of synaptic contacts per 50 μm dendritic length for the indicated conditions. The number of synapses was quantified by counting the number of VGLUT-1 positive puncta overlapping with Cavβ4-eGFP signal along MAP2-positive neuronal processes per 50 μm length. Lines represent the average value ± standard error of the mean (SEM). n.s, not significant. Scale bar: 10 μm.

To investigate whether the $Ca_V\beta_{4b}$-mediated increase in mEPCS frequency depends on the integrity of the actin cytoskeleton, hippocampal neurons were exposed to the actin filament disruptor cytochalasin D prior to the electrophysiological recordings (**Figure 4**). Disruption of the actin cytoskeleton fully abolished the increase in the mEPSC frequency induced by $\beta_{4\text{-WT}}$ (**Figures 4A,B**). Our biochemical analysis indicates that the lack of effect observed for $\beta_{4\text{-Mut}}$ is not due to an impaired F-actin association (**Figure 1C**). Cytochalasin D treatment did not alter the mEPSC frequency in non-transduced neurons (untreated 1.4 ± 0.12 Hz; cytochalasin D-treated 1.17 ± 0.17 Hz, **Figures 4A,B**) suggesting that the actin cytoskeleton does not act as a barrier for spontaneous SV fusion (Sankaranarayanan et al., 2003).

The average mEPSCs decay time in non-transduced neurons was significantly increased after exposure to cytochalasin D (from 0.38 ± 0.03 ms to 0.61 ± 0.06 ms in untreated and cytochalasin D-treated neurons, respectively; **Figure 4C**).

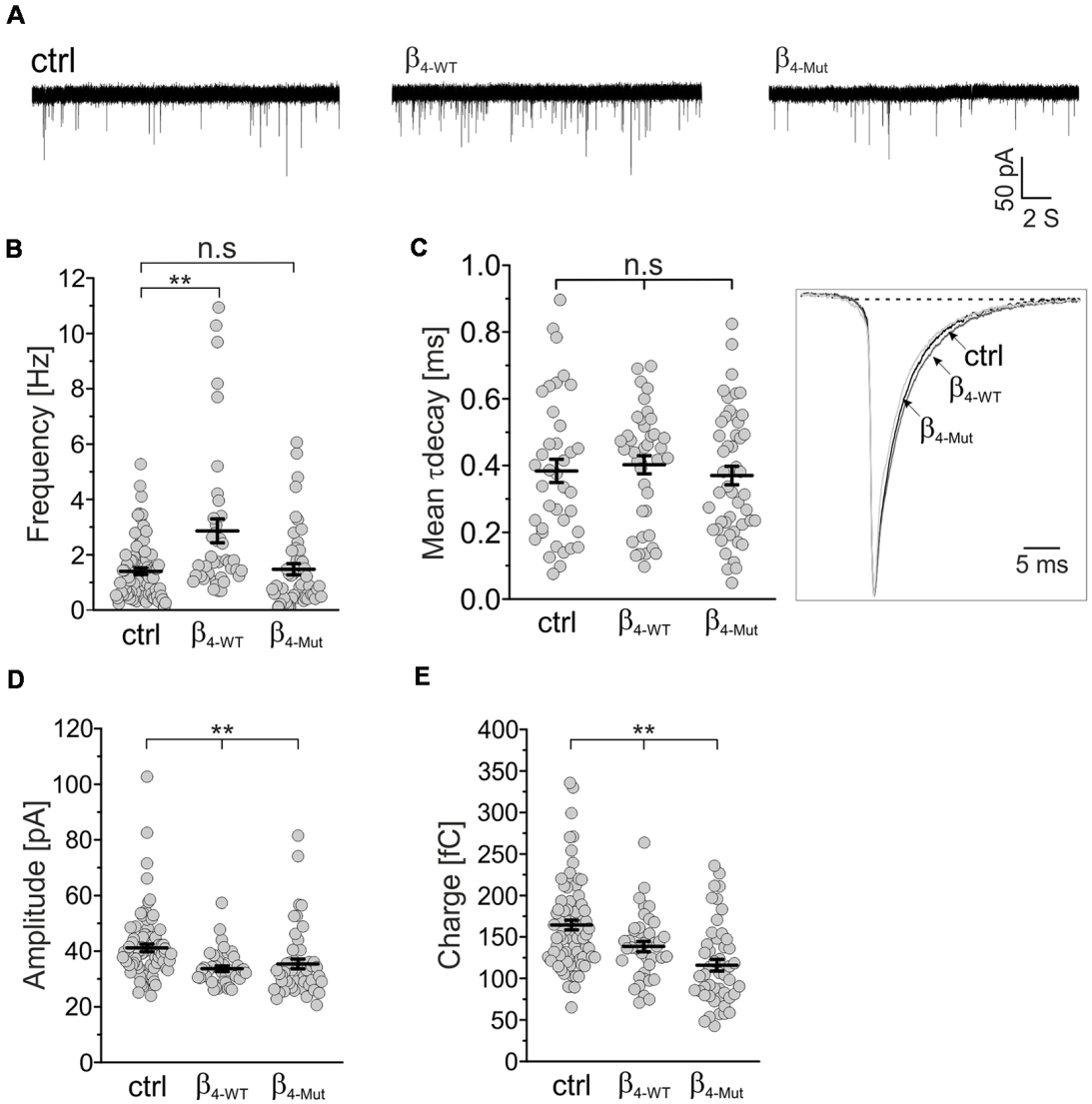

FIGURE 3 | The frequency of excitatory spontaneous release is potentiated only by $Ca_v\beta_4$ bearing an available $Ca_v\alpha_1$-binding site. **(A)** Representative traces of the miniature excitatory spontaneous postsynaptic currents (mEPSCs) from hippocampal neurons in mass cultures non-transduced (ctrl) or transduced with either $\beta_{4\text{-WT}}$ or the $Ca_v\alpha_1$ association-deficient mutant, $\beta_{4\text{-Mut}}$. **(B)** Statistical analysis of mEPSC frequency in control neurons and neurons transduced with either $\beta_{4\text{-WT}}$ or $\beta_{4\text{-Mut}}$. **(C)** Scatter dot plot of the mean weighted decay time (mean τ decay, left panel) for all the tested conditions as indicated for **(A)** and ensemble averages of the normalized mEPSCs (right panel). **(D)** Scatter dot plot of the mEPSC amplitude recorded from control neurons and neurons overexpressing $\beta_{4\text{-WT}}$ and $\beta_{4\text{-Mut}}$. **(E)** Scatter dot plot of the mEPSC charge transfer estimated for the indicated conditions. Lines represent the average value ± SEM. n.s, not significant; $^{**}p < 0.01$ one-way ANOVA.

This is consistent with the notion that actin filaments participate in the spatial organization of the postsynaptic receptors at synapses (Okamoto et al., 2004). Minor changes in the amplitude and charge transfer of the spontaneous response where observed when comparing untreated neurons with their corresponding cytochalasin D-treated counterparts (**Figures 4D,E** and **Supplementary Figures S3C,D**). Nevertheless, a more pronounced effect was found in neurons expressing $\beta_{4\text{-Mut}}$, where the charge transfer decreased from 116 ± 7 fC to 102 ± 6 fC after disruption of the actin cytoskeleton.

Our results show that spontaneous neurotransmitter release is regulated by $Ca_V\beta_{4b}$ and that this regulation relies on an intact actin cytoskeleton and competent binding to $Ca_V\alpha_1$.

A Tripartite Interaction Among $Ca_V\beta$, $Ca_V\alpha_1$ and F-Actin Increases Excitatory Postsynaptic Currents Induced by Depolarization in Hippocampal Neurons

We next recorded evoked EPSCs from autaptic cultures of dissociated hippocampal neurons expressing either $\beta_{4\text{-WT}}$ or

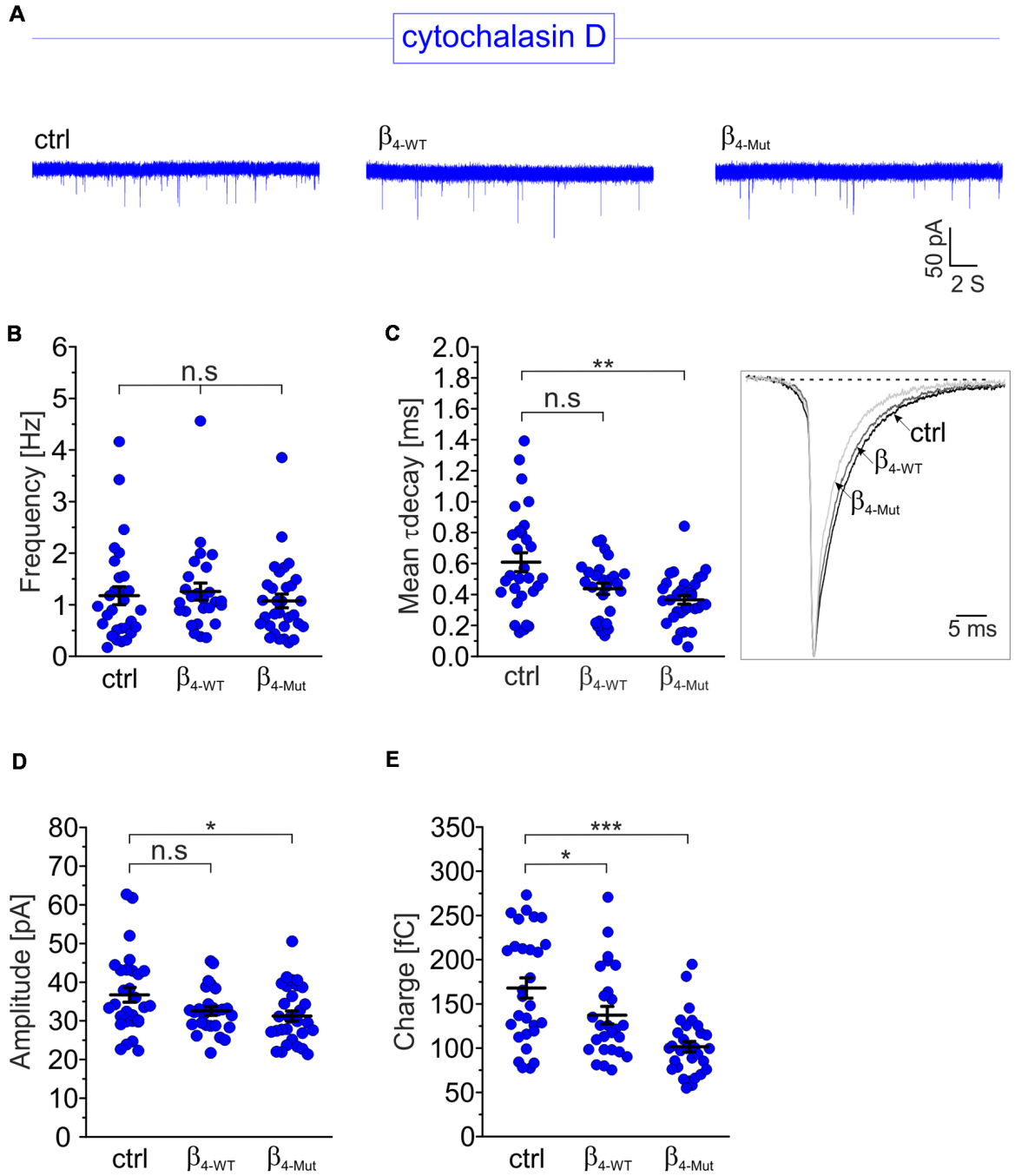

FIGURE 4 | The enhancement of the mEPSC frequency induced by exogenous $Ca_V\beta_{4b}$ relies on a competent actin cytoskeleton. **(A)** Representative traces of mEPSC from neurons exposed to the cytochalasin D actin filament disruptor for 1 h (20 μM). For clarity, traces and plots from non-transduced neurons (ctrl) and transduced with either $\beta_{4\text{-WT}}$ or $\beta_{4\text{-Mut}}$ exposed to cytochalasin D are shown in blue in all figures. **(B)** Statistical analysis of mEPSC frequency for neurons exposed to cytochalasin D as shown in **(A)**. **(C)** Scatter dot plot of the mean weighted decay time (mean τ decay, left panel) and ensemble averages of the mEPSCs (right panel) from the neurons exposed to cytochalasin D for the indicated conditions. **(D)** Scatter dot plot of the mEPSC amplitude recorded from the indicated neurons treated with cytochalasin D. **(E)** Scatter dot plot of the mEPSC charge transfer estimated for the indicated conditions. Lines represent the average value ± SEM. n.s, not significant; $^*p < 0.05$, $^{**}p < 0.01$, $^{***}p < 0.001$ one-way ANOVA.

$\beta_{4\text{-Mut}}$ (**Figure 5**). Consistent with previous work (Wittemann et al., 2000; Xie et al., 2007), we observed that exogenous $\beta_{4\text{-WT}}$ resulted in significantly larger amplitudes of the evoked postsynaptic response and increased charge transfer (**Figures 5A,B,D**). The half-width of the averaged EPSCs were unaffected (**Supplementary Figure S4A**). Expression of $\beta_{4\text{-Mut}}$

caused no changes in the amplitude, charge transfer and kinetics of the EPSCs (**Figures 5A,B,D** and **Supplementary Figure S4A**). Comparison of the EPSCs amplitudes from day 10–14 DIV showed no significant changes suggesting that during this time window, exogenous $\beta_{4\text{-Mut}}$ has reached equilibrium with its endogenous counterparts (data not shown). Moreover, during the same time window, it does affect the RRP size, as shown below. Thus, we do not attribute the lack of effect of $\beta_{4\text{-Mut}}$ to a failure in its ability to actively displace endogenous $Ca_V\beta_4$.

To assess the impact of the actin cytoskeleton, we exposed hippocampal autaptic cultures expressing either $\beta_{4\text{-WT}}$ or $\beta_{4\text{-Mut}}$ to cytochalasin D before recording the postsynaptic currents. Cytochalasin D treatment did not change the amplitude, charge transfer or kinetics of the evoked EPSC response in non-transduced neurons, but blunted the effect of $\beta_{4\text{-WT}}$ on the EPSC amplitude (**Figure 5A**, blue traces and **C–E** and **Supplementary Figure S4B**).

In order to investigate if the effects of cytochalasin D can be mimicked by other actin cytoskeleton disruptor, we treated non-transfected and $\beta_{4\text{-WT}}$-transfected neurons with latrunculin A. We found that this drug also suppressed the increase in EPSC amplitude and charge mediated by $\beta_{4\text{-WT}}$ (**Supplementary Figures S5A,C,D**).

Altogether, our findings demonstrate that a tripartite interaction among $Ca_V\beta$, $Ca_V\alpha_1$ and F-actin upregulates spontaneous and depolarization-evoked neurotransmitter release *via* activation of presynaptic mechanisms. The requirement of an intact actin cytoskeleton for the increase in synaptic strength regulated by $Ca_V\beta_{4b}$ recalls the role of F-actin in mobilizing SVs at different steps of the SV cycle (Cingolani and Goda, 2008).

$Ca_V\beta_4$ Increases the Mobilization of Synaptic Vesicles to the Readily Releasable Pool in an F-Actin Dependent Manner

To test whether $Ca_V\beta$/F-actin association is involved in SV translocation, we estimated the size of the RRP. To compare the impact of WT and mutant $Ca_V\beta_{4b}$ *per se*, and not due to calcium-dependent effects, we use hypertonic sucrose stimulation that is well-established strategy to measure the RRP size in a calcium-independent manner (Rosenmund and Stevens, 1996). The RRP size was measured 5 s after recording the depolarization-evoked response in the same autaptic neuron (**Figure 6**). Neurons transfected with $\beta_{4\text{-WT}}$ and $\beta_{4\text{-Mut}}$ displayed an augmented overall RRP size (**Figures 6A,B**). To assess whether or not our measurements of the RRP size in $Ca_V\beta_4$-expressing neurons were affected by postsynaptic receptor saturation, we estimated the size of the RRP in neurons expressing $\beta_{4\text{-WT}}$ in the presence and in the absence of 1 mM γ–D-Glutamylglycine, a fast dissociating AMPA receptor antagonist (Liu et al., 1999). The result demonstrated that in our study, postsynaptic receptor saturation does not contribute to the RRP size measurements (**Supplementary Figure S6**). This is consistent with the previous report using another AMPA receptor antagonist (Schotten et al., 2015). Postsynaptic receptor desensitization contributing to RRP estimations using 500 mM sucrose solution in hippocampal neurons has been negligible (Pyott and Rosenmund, 2002).

In non-transduced neurons, the pharmacological disruption of the actin cytoskeleton led to a reduction in the average of the RRP size (**Figure 6A**, blue traces, and **C**). Thus, cytochalasin D sensitive actin filaments appear to facilitate, rather than hamper the mobilization of SVs to the RRP under resting conditions.

In neurons transduced with either $\beta_{4\text{-WT}}$ or $\beta_{4\text{-Mut}}$, pharmacological disruption of actin filaments by either cytochalasin D or latrunculin A blunted the increase in the RRP size triggered by this subunit (**Figures 6A,C** and **Supplementary Figures S5B,E**). Cytochalasin D-treatment was less efficient in inhibiting the increased RRP size mediated by $\beta_{4\text{-Mut}}$ (**Figure 6C**). The remaining cytochalasin D-insensitive pool of mobilized SVs may reflect a cluster of remote vesicles that escape the actin network surrounding the active zone.

The Recovery of the RRP Size After Depletion Is Facilitated by $Ca_V\beta_4$ Through a $Ca_V\alpha_1$-Dependent Binding and Is Tightly Controlled by F-Actin

Finally, we investigated if the interaction between $Ca_V\beta_4$ and F-actin also affects the time course of the RRP recovery after depletion (**Figure 7**). In control autaptic neurons and neurons expressing the $Ca_V\alpha_1$ association-deficient mutant subunit, the RRP is replenished with a time constant of about 12 s (**Figures 7A,C,E**), which is consistent with the literature (Stevens and Tsujimoto, 1995). However, $\beta_{4\text{-WT}}$ greatly reduces the time constant for the vesicular replenishment of the RRP (τ_{rec} = 5.7 ± 0.9 s as compared to τ_{rec} = 12.3 ± 2.0 s from non-transduced and τ_{rec} = 12.3 ± 2.6 s for neurons transduced with $\beta_{4\text{-Mut}}$). Pharmacological treatment of the neurons with cytochalasin D reverted the effect of the WT subunit and yielded comparable rates of the RRP recovery time among the three groups of neurons, non-transduced and transduced with either $\beta_{4\text{-WT}}$ or $\beta_{4\text{-Mut}}$ (**Figures 7B,D,F**). These results indicate that the association of $Ca_V\beta_{4b}$ with $Ca_V\alpha_1$ and cytochalasin D-sensitive F-actin accelerates the recovery of the RRP after depletion.

DISCUSSION

We here show that the changes in synaptic transmission elicited by $Ca_V\beta_{4b}$ in hippocampal neurons at excitatory synapses are mediated by actin filaments and involve presynaptic mobilization and maturation of SVs toward a fusion-competent state. Direct comparison of the effects of the WT $Ca_V\beta_{4b}$ and the $Ca_V\alpha_1$ association-deficient mutant on neurotransmission allowed us to define a novel channel-independent function of this subunit in recruiting vesicles to the RRP.

The Functional Interplay Among $Ca_V\alpha$, $Ca_V\beta$ and F-Actin Regulates Synaptic Transmission

Several roles of the actin cytoskeleton at the presynaptic terminal have been considered (Morales et al., 2000;

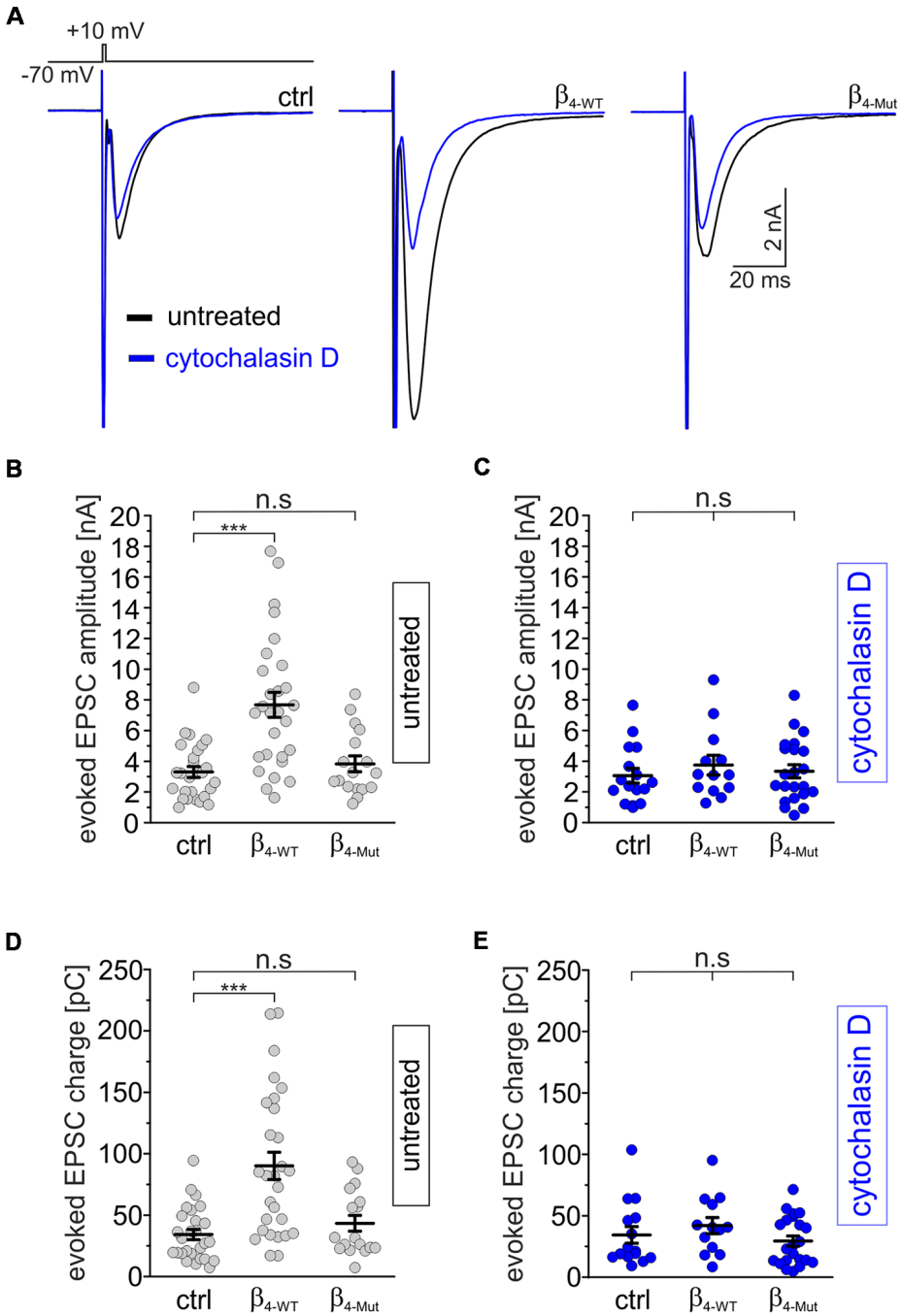

FIGURE 5 | The tripartite interaction among $Ca_V\beta$, $Ca_V\alpha_1$ and F-actin is required for increasing depolarization-evoked EPSCs in individual hippocampal neurons. **(A)** Averaged EPSC response from autaptic hippocampal neurons evoked with the voltage protocol shown at the top. Overlapped average EPSC responses from neurons non-exposed (untreated, black traces) and exposed to 20 μM cytohalasin D for 1 h (blue traces) and expressing either $\beta_{4\text{-WT}}$ or $\beta_{4\text{-Mut}}$ or non-transduced (ctrl) are shown. **(B,C)** Scatter dot plots of the EPSCs amplitude recorded from untreated neurons and cytochalasin D-treated neurons, respectively. **(D,E)** Scatter dot plots of the EPSCs charge transfer estimated from untreated and cytochalasin-D treated neurons, respectively. Lines represent the average value ± SEM. n.s, not significant; ***$p < 0.001$ one-way ANOVA.

Cingolani and Goda, 2008; Choquet and Triller, 2013; Nelson et al., 2013; Rust and Maritzen, 2015). Actin filaments may serve as tracks for the active translocation of SVs in synaptic terminals or as a scaffold to recruit and promote the interaction of regulatory proteins required for neurotransmitter release. They may also act as a barrier for SV mobilization toward the release site (Halpain, 2003; Sankaranarayanan et al., 2003; Miki et al., 2016).

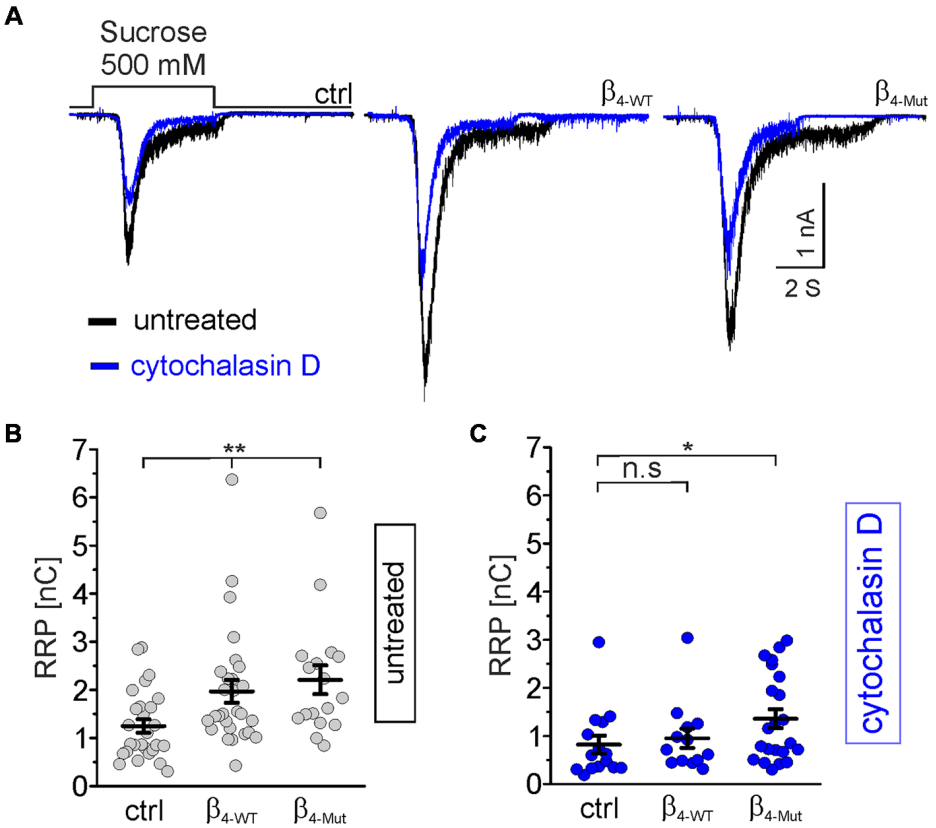

FIGURE 6 | $Ca_V\beta_4$ WT, as well as the $Ca_V\alpha_1$ association-deficient mutant, increases the readily releasable pool (RRP) of synaptic vesicles (SVs) in an F-actin dependent manner. **(A)** Representative whole-cell responses to hypertonic sucrose solution stimulation (500 mM sucrose) from autaptic non-transduced neurons and either transduced with $\beta_{4\text{-WT}}$ or $\beta_{4\text{-Mut}}$. The responses from untreated neurons and cytochalasin D-treated neurons were overlapped and are shown in black and blue traces, respectively. **(B,C)** Scatter dot plots of the RRP size from untreated and cytochalasin D-treated neurons, respectively. Lines represent the average value ± SEM. n.s, not significant; $^*p < 0.05$, $^{**}p < 0.01$ one-way ANOVA.

The increased mean decay time of the miniature response following cytochalasin D-treatment (**Figure 4C**) is most likely due to the involvement of the actin cytoskeleton on the spatial arrangement of the postsynaptic receptors (Okamoto et al., 2004). Disruption of the actin cytoskeleton with cytochalasin D *per se* did not alter the frequency of the miniature response or the amplitude of the depolarization-evoked EPSC response in non-transfected neurons but prevented their potentiation triggered by exogenous $Ca_V\beta_4$. Comparable results on evoked response were obtained when actin polymerization was inhibited with latrunculin A (**Supplementary Figure S5**).

The lack of effect of F-actin disruption on non-transfected hippocampal neurons has been suggested to reflect a counteracting effect between the two opposing presynaptic roles attributed to the actin cytoskeleton; as a barrier as well as a facilitator for the mobilization of SVs (Cingolani and Goda, 2008). Within this framework, our observation that cytochalasin D treatment decreased the RRP size (**Figure 6**) implies that under our conditions, F-actin acts predominantly as an entryway to repopulate the RRP (Wu et al., 2016).

The tripartite interaction would acquire physiological relevance during high synaptic activity whereby efficient coupling between SVs and $Ca_V\alpha_1$ (and upregulation of the RRP size and their replenishment rate) is required. Enhanced neurotransmission mediated by $Ca_V\beta$/F-actin association would rely on higher availability of this subunit to be rerouted toward this function. In other words, the accessibility of this subunit may be a key determinant for regulating synaptic strength *via* F-actin cytoskeleton and may constitute a rate-limiting step for neurotransmission adaptation in response to the increased activity *via* F-actin association.

Whether spontaneous vesicle release depends on $Ca_V2.x$-mediated calcium influx (Kaeser and Regehr, 2014; Williams and Smith, 2018) and whether the same pool of SVs (Groemer and Klingauf, 2007; Ikeda and Bekkers, 2009) or a distinct subset (Fredj and Burrone, 2009) is dedicated to miniature and evoked neurotransmitter release remains under discussion (for review, Truckenbrodt and Rizzoli, 2014). In spite of the controversy, our results demonstrate that the increased frequency of spontaneous release depends on a competent F-actin and intact $Ca_V\alpha_1$ binding site suggesting that close proximity of SVs to $Ca_V\alpha_1$ is required. This requirement may reflect a dependence of the spontaneous release on calcium permeation through $Ca_V2.x$ channels. In such a case,

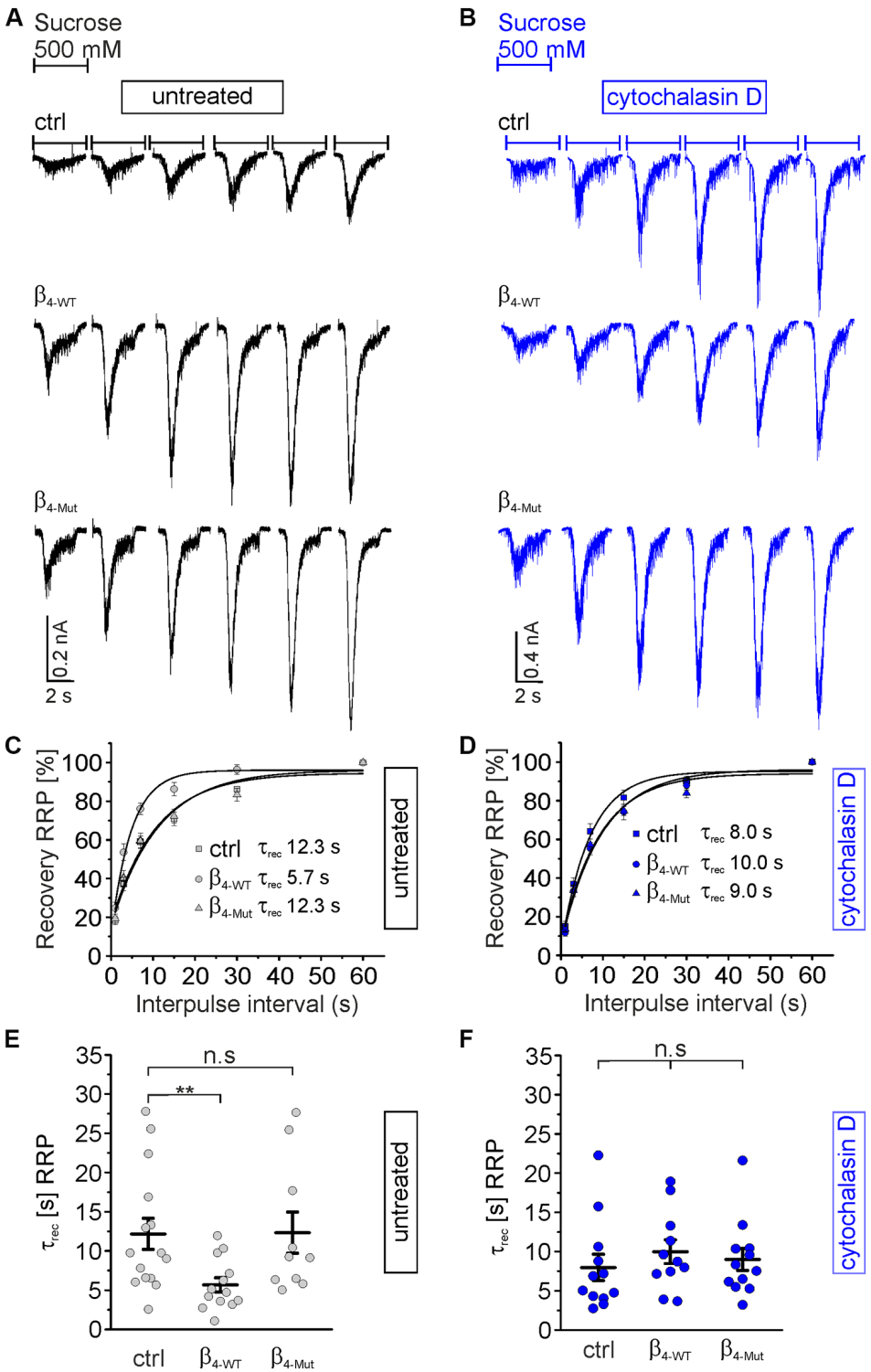

FIGURE 7 | $Ca_V\alpha_1$-binding confers $Ca_V\beta_4$ the ability to accelerate the time course of recovery of the RRP of SVs after depletion. **(A)** Representative recordings of sucrose responses at increasing time points after depletion from autaptic hippocampal neurons expressing or not the indicated $Ca_V\beta$ constructs. **(B)** Representative recordings of sucrose responses as **(A)** but for neurons exposed to cytochalasin D. **(C,D)** Average recovery time course of the RRP replenishment after depletion from data as shown in **(A,B)**, respectively. Continuous lines depict monoexponential fits, and the corresponding time constants (τ_{rec}) are reported in the graph. **(E,F)** Scatter dot plot of τ_{rec} from the individual untreated neurons and treated with cytochalasin D, respectively. Lines represent the average value ± SEM. n.s, not significant; $^{**}p < 0.01$ one-way ANOVA.

$Ca_V\beta$/F-actin association tethers SV to the channel complex and promotes spontaneous release upon stochastic channel opening (Ermolyuk et al., 2013). The finding that the same tripartite interaction, $Ca_V\beta$, F-actin and $Ca_V\alpha_1$, is required for the increased evoked response supports the concept of an overlapping pool of vesicles and release sites, which mediates these two modes of neurotransmission.

We propose that the tripartite interaction is mandatory for generating a fusion-competent SV by allowing the coupling of primed SVs with the calcium channel at the release site. $Ca_V\beta_4$ mutant with no capability to associate with $Ca_V\alpha_1$ (**Supplementary Figure S2**) fails in tethering the SV to the calcium channel and explains the lack of effect of the mutant $Ca_V\beta_4$ on the frequency of the spontaneous neurotransmitter release and evoked response.

$Ca_V\beta_4$/F-Actin Interaction Recruits Synaptic Vesicles to the Readily Releasable Pool and Is Involved in Its Replenishment

We found that both tested $Ca_V\beta$s—WT and mutant without the ability to associate with $Ca_V\alpha_1$—support the recruitment of SVs to the RRP in concert with F-actin (**Figure 6**). Thus, the $Ca_V\beta$-regulated increase in the RRP size operates independently of $Ca_V\alpha_1$ function. This is in line with the idea that neurotransmitter release evoked by hypertonic sucrose solution in hippocampal neurons is independent of calcium (Rosenmund and Stevens, 1996). Our results differ from a previous study, which reported unaltered RRP size in hippocampal neurons overexpressing $Ca_V\beta_4$ and accelerated RRP recovery only after train stimulation. These studies suggested that the latter arose from an increased calcium influx (Xie et al., 2007). We believe that these differences are due to the use of two distinct $Ca_V\beta_4$ fusion constructs; whereas we linked eGFP to the C-terminus of the β-subunit, the authors of the other study attached the GFP to the N-terminus. The SH3 domain located at the N-terminal moiety of the protein is a main determinant of F-actin binding (Stölting et al., 2015), and N-terminal fusion might have masked functionally relevant protein-protein interactions.

The capability of $Ca_V\beta_4$ to increase the RRP size hints to a direct role of this subunit in the translocation of vesicles along F-actin (Evans et al., 1998; Cingolani and Goda, 2008; Rust and Maritzen, 2015). This subunit may accumulate in the actin network surrounding SVs at the synaptic terminal and aid their passive recruitment to the RRP or their active trafficking along actin filaments by yet to be established protein-protein interactions. In analogy, $Ca_V\beta$/F-actin association appears to recruit $Ca_V1.2$-containing transport vesicles nearby the plasma membrane for recycling in cardiac cells (Stölting et al., 2015; Conrad et al., 2018).

In excitatory hippocampal neurons, SVs within the RRP differ in their readiness to release their content upon a depolarizing stimulus (Hanse and Gustafsson, 2001; Moulder and Mennerick, 2005, 2006; Alabi and Tsien, 2012; Taschenberger et al., 2016; Kaeser and Regehr, 2017). Moreover, reluctant SVs can be converted into fast-releasing ones in an actin-dependent manner by bringing SVs closer to Ca_V channels, supporting the so-called positional priming hypothesis (Lee et al., 2012). Within this context, our results are consistent with the notion that $Ca_V\beta$ mutant mobilizes a subset of reluctant vesicles to the RRP whereas the WT protein translocate vesicles to the RRP and through its ability to associate with $Ca_V\alpha_1$ renders SV fusion competent.

Diverse protein-protein interactions are involved in positioning SVs and Ca_Vs within nanometer distance at the release site (Eggermann et al., 2011; Davydova et al., 2014; Gundelfinger et al., 2015; Nakamura et al., 2015; Korber and Kuner, 2016; Stanley, 2016; Wang et al., 2016; Kusch et al., 2018; de Jong et al., 2018). Among those, the multi-domain RIM associates directly with $Ca_V2.x$ channels (Hibino et al., 2002). It has been reported that $Ca_V\beta$ also interacts with RIM (Kiyonaka et al., 2007) as well as with synaptotagmin I (Vendel et al., 2006). We here show that $Ca_V\beta_4$ can simultaneously associate with F-actin and $Ca_V\alpha_1$. This interplay may provide a molecular scaffold to hold in place the plethora of proteins involved in SV docking and priming. Moreover, the dimerization of $Ca_V\beta$ (Miranda-Laferte et al., 2011) may also enlarge the number of potential interacting partners regulating synaptic activity. The idea that $Ca_V\beta$ may operate as a scaffold between the calcium channel and the release machinery has been anticipated (Vendel et al., 2006; Weiss, 2006; Xie et al., 2007).

$\beta_{4\text{-Mut}}$ preserves its ability to associate with F-actin and to recruit SVs to the RRP but fails to speed up the recovery time of the RRP after depletion. The RRP replenishment was measured following calcium-independent exocytosis so that this lack of effect is not due to its inability to increase calcium current densities. As acceleration of RRP recovery relies on a $Ca_V\beta_4$ with intact $Ca_V\alpha_1$-binding site, fast replenishment appears to be acquired only after the SV is tethered to $Ca_V\alpha_1$. One can envision that a set of molecular components that prepares the SV and the release site for undergoing fast retrieval is recruited after positioning the SV in close proximity to the calcium channel.

Multiple lines of evidence and theoretical insight agree with the concept that clearance of the release site, rather than SV supply, becomes rate limiting during sustained neurotransmission (Neher, 2010). Regeneration of SVs by the classical clathrin-mediated endocytosis is too slow to account for the effect of $Ca_V\beta_4$ on the RRP replenishment (Granseth et al., 2007; Granseth and Lagnado, 2008; Yamashita, 2012). Recently, a clathrin-independent ultrafast endocytosis within 50–100 ms after exocytosis was reported in mouse hippocampal neurons (Watanabe et al., 2013, 2014). It occurs at regions flanking the active zone and depends on F-actin and dynamin, two interacting partners of $Ca_V\beta$. Ultrafast endocytosis could primarily serve fast, compensatory retrieval of vesicular membranes and would be followed by the formation of large vesicles that fuse with endosomes and reform a functional SV through a clathrin-dependent process with a much slower time scale in the order of seconds.

Actin appears to mediate virtually all types of SV endocytosis and to facilitate translocation of SVs to the RRP (Wu et al., 2016). Likewise, dynamin is required for the fission of the SV at the cost of GTP hydrolysis and suggested to participate in

the clearance of the release sites in different model systems, including hippocampal neurons (Kawasaki et al., 2000; Hosoi et al., 2009; Wu et al., 2009; Soykan et al., 2017). It is recruited to endocytic sites *via* interaction with several proteins containing SH-3 domains. We have previously shown that $Ca_V\beta$ interacts with dynamin *via* its SH3 domain and promotes endocytosis (Gonzalez-Gutierrez et al., 2007; Miranda-Laferte et al., 2011). It is tempting to propose that $Ca_V\beta_4$ facilitates RRP replenishment by promoting dynamin/F-actin-dependent endocytosis that speeds up the removal of SV components and excess of membrane for a new cycle of release at the release site after exocytosis. Since undersupply of SVs and cleared release sites can cause transient synaptic depression during high synaptic activity, upregulation of the RRP size and their replenishment mediated by exogenous $Ca_V\beta$/F-actin association would support stable neurotransmission during sustained synaptic activity.

In conclusion, a physical association between $Ca_V\beta_4$, $Ca_V\alpha_1$ and F-actin appears to be a sine-qua-non condition for bringing the SV within the permissive range of the Ca_V calcium nanodomain for release (Naraghi and Neher, 1997; Neher and Sakaba, 2008; Park et al., 2012; Nakamura et al., 2015; Stanley, 2015, 2016). This scenario places $Ca_V\beta_4$ as essential for the maturation of the SVs toward a fusion-competent state acting as a tether for the functional priming of the SV during spontaneous and depolarization-evoked synaptic transmission.

ETHICS STATEMENT

This study was carried out in accordance with the recommendations of the German Law for the Protection of Animals. The protocol was approved by the Forschungszentrum Jülich GmbH and LANUV (State Agency for Nature, Environment and Consumer Protection) of North Rhine-Westphalia.

AUTHOR CONTRIBUTIONS

GG designed and performed the experiments, analyzed the data and edited the manuscript. RG analyzed data and edited manuscript. NJ produced all recombinant proteins and performed the biochemical assays and immunostainings. PH designed and supervised the research, and wrote the article.

FUNDING

This work was supported by Research Center Jülich (Forschungszentrum Jülich).

ACKNOWLEDGMENTS

We are very grateful for all the discussions and support of Christoph Fahlke throughout this work and for the excellent technical assistance in molecular biology of Arne Franzen and Petra Thelen.

SUPPLEMENTARY MATERIAL

The Supplementary Material for this article can be found online at: https://www.frontiersin.org/articles/10.3389/fncel.2019.00125/full#supplementary-material

REFERENCES

Alabi, A. A., and Tsien, R. W. (2012). Synaptic vesicle pools and dynamics. *Cold Spring Harb. Perspect. Biol.* 4:a013680. doi: 10.1101/cshperspect.a013680

Barde, I., Salmon, P., and Trono, D. (2010). Production and titration of lentiviral vectors. *Curr. Protoc. Neurosci.* Chapter 12:Unit 12.10. doi: 10.1002/0471142301.ns0421s53

Blondeau, F., Ritter, B., Allaire, P. D., Wasiak, S., Girard, M., Hussain, N. K., et al. (2004). Tandem MS analysis of brain clathrin-coated vesicles reveals their critical involvement in synaptic vesicle recycling. *Proc. Natl. Acad. Sci. U S A* 101, 3833–3838. doi: 10.1073/pnas.0308186101

Buraei, Z., and Yang, J. (2010). The β-subunit of voltage-gated Ca^{2+} channels. *Physiol. Rev.* 90, 1461–1506. doi: 10.1152/physrev.00057.2009

Cao, Y. Q., and Tsien, R. W. (2010). Different relationship of N- and P/Q-type Ca^{2+} channels to channel-interacting slots in controlling neurotransmission at cultured hippocampal synapses. *J. Neurosci.* 30, 4536–4546. doi: 10.1523/JNEUROSCI.5161-09.2010

Chen, Y. H., Li, M. H., Zhang, Y., He, L. L., Yamada, Y., Fitzmaurice, A., et al. (2004). Structural basis of the α_1-β subunit interaction of voltage-gated Ca^{2+} channels. *Nature* 429, 675–680. doi: 10.1038/nature02641

Choquet, D., and Triller, A. (2013). The dynamic synapse. *Neuron* 80, 691–703. doi: 10.1016/j.neuron.2013.10.013

Cingolani, L. A., and Goda, Y. (2008). Actin in action: the interplay between the actin cytoskeleton and synaptic efficacy. *Nat. Rev. Neurosci.* 9, 344–356. doi: 10.1038/nrn2373

Conrad, R., Stölting, G., Hendriks, J., Ruello, G., Kortzak, D., Jordan, N., et al. (2018). Rapid turnover of the cardiac L-Type $Ca_V1.2$ channel by endocytic recycling regulates its cell surface availability. *Science* 7, 1–15. doi: 10.1016/j.isci.2018.08.012

Davydova, D., Marini, C., King, C., Klueva, J., Bischof, F., Romorini, S., et al. (2014). Bassoon specifically controls presynaptic P/Q-type Ca^{2+} channels via RIM-binding protein. *Neuron* 82, 181–194. doi: 10.1016/j.neuron.2014.02.012

de Jong, A. P. H., Roggero, C. M., Ho, M. R., Wong, M. Y., Brautigam, C. A., Rizo, J., et al. (2018). RIM C2B domains target presynaptic active zone functions to PIP2-containing membranes. *Neuron* 98, 335.e7–349.e7. doi: 10.1016/j.neuron.2018.03.011

Eggermann, E., Bucurenciu, I., Goswami, S. P., and Jonas, P. (2011). Nanodomain coupling between Ca^{2+} channels and sensors of exocytosis at fast mammalian synapses. *Nat. Rev. Neurosci.* 13, 7–21. doi: 10.1038/nrn3125

Ermolyuk, Y. S., Alder, F. G., Surges, R., Pavlov, I. Y., Timofeeva, Y., Kullmann, D. M., et al. (2013). Differential triggering of spontaneous glutamate release by P/Q-, N- and R-type Ca^{2+} channels. *Nat. Neurosci.* 16, 1754–1763. doi: 10.1038/nn.3563

Etemad, S., Obermair, G. J., Bindreither, D., Benedetti, A., Stanika, R., Di Biase, V., et al. (2014). Differential neuronal targeting of a new and two known calcium channel β_4 subunit splice variants correlates with their regulation of gene expression. *J. Neurosci.* 34, 1446–1461. doi: 10.1523/JNEUROSCI.3935-13.2014

Evans, L. L., Lee, A. J., Bridgman, P. C., and Mooseker, M. S. (1998). Vesicle-associated brain myosin-V can be activated to catalyze actin-based transport. *J. Cell Sci.* 111, 2055–2066.

Fredj, N. B., and Burrone, J. (2009). A resting pool of vesicles is responsible for spontaneous vesicle fusion at the synapse. *Nat. Neurosci.* 12, 751–758. doi: 10.1038/nn.2317

Gonzalez-Gutierrez, G., Miranda-Laferte, E., Neely, A., and Hidalgo, P. (2007). The Src homology 3 domain of the β-subunit of voltage-gated calcium channels promotes endocytosis via dynamin interaction. *J. Biol. Chem.* 282, 2156–2162. doi: 10.1074/jbc.m609071200

Granseth, B., and Lagnado, L. (2008). The role of endocytosis in regulating the strength of hippocampal synapses. *J. Physiol.* 586, 5969–5982. doi: 10.1113/jphysiol.2008.159715

Granseth, B., Odermatt, B., Royle, S. J., and Lagnado, L. (2007). Clathrin-mediated endocytosis: the physiological mechanism of vesicle retrieval at hippocampal synapses. *J. Physiol.* 585, 681–686. doi: 10.1113/jphysiol.2007.139022

Groemer, T. W., and Klingauf, J. (2007). Synaptic vesicles recycling spontaneously and during activity belong to the same vesicle pool. *Nat. Neurosci.* 10, 145–147. doi: 10.1038/nn1831

Gundelfinger, E. D., Reissner, C., and Garner, C. C. (2015). Role of bassoon and piccolo in assembly and molecular organization of the active zone. *Front. Synaptic Neurosci.* 7:19. doi: 10.3389/fnsyn.2015.00019

Guzman, R. E., Schwarz, Y. N., Rettig, J., and Bruns, D. (2010). SNARE force synchronizes synaptic vesicle fusion and controls the kinetics of quantal synaptic transmission. *J. Neurosci.* 30, 10272–10281. doi: 10.1523/JNEUROSCI.1551-10.2010

Hallermann, S., and Silver, R. A. (2013). Sustaining rapid vesicular release at active zones: potential roles for vesicle tethering. *Trends Neurosci.* 36, 185–194. doi: 10.1016/j.tins.2012.10.001

Halpain, S. (2003). Actin in a supporting role. *Nat. Neurosci.* 6, 101–102. doi: 10.1038/nn0203-101

Hanse, E., and Gustafsson, B. (2001). Vesicle release probability and pre-primed pool at glutamatergic synapses in area CA1 of the rat neonatal hippocampus. *J. Physiol.* 531, 481–493. doi: 10.1111/j.1469-7793.2001.0481i.x

Hayashida, M., Tanifuji, S., Ma, H., Murakami, N., and Mochida, S. (2015). Neural activity selects myosin IIB and VI with a specific time window in distinct dynamin isoform-mediated synaptic vesicle reuse pathways. *J. Neurosci.* 35, 8901–8913. doi: 10.1523/JNEUROSCI.5028-14.2015

Hibino, H., Pironkova, R., Onwumere, O., Vologodskaia, M., Hudspeth, A. J., and Lesage, F. (2002). RIM binding proteins (RBPs) couple Rab3-interacting molecules (RIMs) to voltage-gated Ca^{2+} channels. *Neuron* 34, 411–423. doi: 10.1016/s0896-6273(02)00667-0

Hidalgo, P., Gonzalez-Gutierrez, G., Garcia-Olivares, J., and Neely, A. (2006). The α_1-β-subunit interaction that modulates calcium channel activity is reversible and requires a competent α-interaction domain. *J. Biol. Chem.* 281, 24104–24110. doi: 10.1074/jbc.M605930200

Hidalgo, P., and Neely, A. (2007). Multiplicity of protein interactions and functions of the voltage-gated calcium channel β-subunit. *Cell Calcium* 42, 389–396. doi: 10.1016/j.ceca.2007.05.009

Hofmann, F., Belkacemi, A., and Flockerzi, V. (2015). Emerging alternative functions for the auxiliary subunits of the voltage-gated calcium channels. *Curr. Mol. Pharmacol.* 8, 162–168. doi: 10.2174/1874467208666150507110202

Hosoi, N., Holt, M., and Sakaba, T. (2009). Calcium dependence of exo- and endocytotic coupling at a glutamatergic synapse. *Neuron* 63, 216–229. doi: 10.1016/j.neuron.2009.06.010

Ikeda, K., and Bekkers, J. M. (2009). Counting the number of releasable synaptic vesicles in a presynaptic terminal. *Proc. Natl. Acad. Sci. U S A* 106, 2945–2950. doi: 10.1073/pnas.0811017106

Kaeser, P. S., and Regehr, W. G. (2014). Molecular mechanisms for synchronous, asynchronous, and spontaneous neurotransmitter release. *Annu. Rev. Physiol.* 76, 333–363. doi: 10.1146/annurev-physiol-021113-170338

Kaeser, P. S., and Regehr, W. G. (2017). The readily releasable pool of synaptic vesicles. *Curr. Opin. Neurobiol.* 43, 63–70. doi: 10.1016/j.conb.2016.12.012

Kawasaki, F., Hazen, M., and Ordway, R. W. (2000). Fast synaptic fatigue in shibire mutants reveals a rapid requirement for dynamin in synaptic vesicle membrane trafficking. *Nat. Neurosci.* 3, 859–860. doi: 10.1038/78753

Kiyonaka, S., Wakamori, M., Miki, T., Uriu, Y., Nonaka, M., Bito, H., et al. (2007). RIM1 confers sustained activity and neurotransmitter vesicle anchoring to presynaptic Ca^{2+} channels. *Nat. Neurosci.* 10, 691–701. doi: 10.1038/nn1904

Korber, C., and Kuner, T. (2016). Molecular machines regulating the release probability of synaptic vesicles at the active zone. *Front. Synaptic Neurosci.* 8:5. doi: 10.3389/fnsyn.2016.00005

Kusch, V., Bornschein, G., Loreth, D., Bank, J., Jordan, J., Baur, D., et al. (2018). Munc13–3 is required for the developmental localization of Ca^{2+} channels to active zones and the nanopositioning of Cav2.1 near release sensors. *Cell Rep.* 22, 1965–1973. doi: 10.1016/j.celrep.2018.02.010

Lee, J. S., Ho, W. K., and Lee, S. H. (2012). Actin-dependent rapid recruitment of reluctant synaptic vesicles into a fast-releasing vesicle pool. *Proc. Natl. Acad. Sci. U S A* 109, E765–E774. doi: 10.1073/pnas.1114072109

Liu, G., Choi, S., and Tsien, R. W. (1999). Variability of neurotransmitter concentration and nonsaturation of postsynaptic AMPA receptors at synapses in hippocampal cultures and slices. *Neuron* 22, 395–409. doi: 10.1016/s0896-6273(00)81099-5

Miki, T., Malagon, G., Pulido, C., Llano, I., Neher, E., and Marty, A. (2016). Actin- and myosin-dependent vesicle loading of presynaptic docking sites prior to exocytosis. *Neuron* 91, 808–823. doi: 10.1016/j.neuron.2016.07.033

Miranda-Laferte, E., Ewers, D., Guzman, R. E., Jordan, N., Schmidt, S., and Hidalgo, P. (2014). The N-terminal domain tethers the voltage-gated calcium channel β_{2e}-subunit to the plasma membrane via electrostatic and hydrophobic interactions. *J. Biol. Chem.* 289, 10387–10398. doi: 10.1074/jbc.M113.507244

Miranda-Laferte, E., Gonzalez-Gutierrez, G., Schmidt, S., Zeug, A., Ponimaskin, E. G., Neely, A., et al. (2011). Homodimerization of the Src homology 3 domain of the calcium channel β-subunit drives dynamin-dependent endocytosis. *J. Biol. Chem.* 286, 22203–22210. doi: 10.1074/jbc.M110.201871

Morales, M., Colicos, M. A., and Goda, Y. (2000). Actin-dependent regulation of neurotransmitter release at central synapses. *Neuron* 27, 539–550. doi: 10.1016/s0896-6273(00)00064-7

Morciano, M., Burré, J., Corvey, C., Karas, M., Zimmermann, H., and Volknandt, W. (2005). Immunoisolation of two synaptic vesicle pools from synaptosomes: a proteomics analysis. *J. Neurochem.* 95, 1732–1745. doi: 10.1111/j.1471-4159.2005.03506.x

Moulder, K. L., and Mennerick, S. (2005). Reluctant vesicles contribute to the total readily releasable pool in glutamatergic hippocampal neurons. *J. Neurosci.* 25, 3842–3850. doi: 10.1523/JNEUROSCI.5231-04.2005

Moulder, K. L., and Mennerick, S. (2006). Synaptic vesicles: turning reluctance into action. *Neuroscientist* 12, 11–15. doi: 10.1177/1073858405282431

Müller, C. S., Haupt, A., Bildl, W., Schindler, J., Knaus, H. G., Meissner, M., et al. (2010). Quantitative proteomics of the Ca_V2 channel nano-environments in the mammalian brain. *Proc. Natl. Acad. Sci. U S A* 107, 14950–14957. doi: 10.1073/pnas.1005940107

Nakamura, Y., Harada, H., Kamasawa, N., Matsui, K., Rothman, J. S., Shigemoto, R., et al. (2015). Nanoscale distribution of presynaptic Ca^{2+} channels and its impact on vesicular release during development. *Neuron* 85, 145–158. doi: 10.1016/j.neuron.2014.11.019

Nanou, E., and Catterall, W. A. (2018). Calcium channels, synaptic plasticity, and neuropsychiatric disease. *Neuron* 98, 466–481. doi: 10.1016/j.neuron.2018.03.017

Naraghi, M., and Neher, E. (1997). Linearized buffered Ca^{2+} diffusion in microdomains and its implications for calculation of $[Ca^{2+}]$ at the mouth of a calcium channel. *J. Neurosci.* 17, 6961–6973. doi: 10.1523/JNEUROSCI.17-18-06961.1997

Neher, E. (2010). What is rate-limiting during sustained synaptic activity: vesicle supply or the availability of release sites. *Thromb. Res.* 2:144. doi: 10.3389/fnsyn.2010.00144

Neher, E., and Sakaba, T. (2008). Multiple roles of calcium ions in the regulation of neurotransmitter release. *Neuron* 59, 861–872. doi: 10.1016/j.neuron.2008.08.019

Nelson, J. C., Stavoe, A. K., and Colón-Ramos, D. A. (2013). The actin cytoskeleton in presynaptic assembly. *Cell Adh. Migr.* 7, 379–387. doi: 10.4161/cam.24803

Okamoto, K., Nagai, T., Miyawaki, A., and Hayashi, Y. (2004). Rapid and persistent modulation of actin dynamics regulates postsynaptic reorganization underlying bidirectional plasticity. *Nat. Neurosci.* 7, 1104–1112. doi: 10.1038/nn1311

Opatowsky, Y., Chen, C. C., Campbell, K. P., and Hirsch, J. A. (2004). Structural analysis of the voltage-dependent calcium channel β-subunit functional core and its complex with the α_1-interaction domain. *Neuron* 42, 387–399. doi: 10.1016/s0896-6273(04)00250-8

Park, H., Li, Y., and Tsien, R. W. (2012). Influence of synaptic vesicle position on release probability and exocytotic fusion mode. *Science* 335, 1362–1366. doi: 10.1126/science.1216937

Pragnell, M., De Waard, M., Mori, M., Tanabe, T., Snutch, T. P., and Campbell, K. P. (1994). Calcium channel β-subunit binds to a conserved

motif in the I-II cytoplasmic linker of the α_1-subunit. *Nature* 368, 67–70. doi: 10.1038/368067a0

Pyott, S. J., and Rosenmund, C. (2002). The effects of temperature on vesicular supply and release in autaptic cultures of rat and mouse hippocampal neurons. *J. Physiol.* 539, 523–535. doi: 10.1113/jphysiol.2001.013277

Rima, M., Daghsni, M., Fajloun, Z., M'Rad, R., Brusés, J. L., Ronjat, M., et al. (2016). Protein partners of the calcium channel β-subunit highlight new cellular functions. *Biochem. J.* 473, 1831–1844. doi: 10.1042/BCJ20160125

Ronjat, M., Kiyonaka, S., Barbado, M., De Waard, M., and Mori, Y. (2013). Nuclear life of the voltage-gated Cacnb4 subunit and its role in gene transcription regulation. *Channels* 7, 119–125. doi: 10.4161/chan.23895

Rosenmund, C., and Stevens, C. F. (1996). Definition of the readily releasable pool of vesicles at hippocampal synapses. *Neuron* 16, 1197–1207. doi: 10.1016/s0896-6273(00)80146-4

Rust, M. B., and Maritzen, T. (2015). Relevance of presynaptic actin dynamics for synapse function and mouse behavior. *Exp. Cell Res.* 335, 165–171. doi: 10.1016/j.yexcr.2014.12.020

Sankaranarayanan, S., Atluri, P. P., and Ryan, T. A. (2003). Actin has a molecular scaffolding, not propulsive, role in presynaptic function. *Nat. Neurosci.* 6, 127–135. doi: 10.1038/nn1002

Schindelin, J., Arganda-Carreras, I., Frise, E., Kaynig, V., Longair, M., Pietzsch, T., et al. (2012). Fiji: an open-source platform for biological-image analysis. *Nat. Methods* 9, 676–682. doi: 10.1038/nmeth.2019

Schotten, S., Meijer, M., Walter, A. M., Huson, V., Mamer, L., Kalogreades, L., et al. (2015). Additive effects on the energy barrier for synaptic vesicle fusion cause supralinear effects on the vesicle fusion rate. *Elife* 4:e05531. doi: 10.7554/elife.05531

Simms, B. A., and Zamponi, G. W. (2014). Neuronal voltage-gated calcium channels: structure, function, and dysfunction. *Neuron* 82, 24–45. doi: 10.1016/j.neuron.2014.03.016

Soykan, T., Kaempf, N., Sakaba, T., Vollweiter, D., Goerdeler, F., Puchkov, D., et al. (2017). Synaptic vesicle endocytosis occurs on multiple timescales and is mediated by formin-dependent actin assembly. *Neuron* 93, 854.e4–866.e4. doi: 10.1016/j.neuron.2017.02.011

Stanley, E. F. (2015). Single calcium channel domain gating of synaptic vesicle fusion at fast synapses; analysis by graphic modeling. *Channels* 9, 324–333. doi: 10.1080/19336950.2015.1098793

Stanley, E. F. (2016). The nanophysiology of fast transmitter release. *Trends Neurosci.* 39, 183–197. doi: 10.1016/j.tins.2016.01.005

Stevens, C. F., and Sullivan, J. M. (1998). Regulation of the readily releasable vesicle pool by protein kinase C. *Neuron* 21, 885–893. doi: 10.1016/s0896-6273(00)80603-0

Stevens, C. F., and Tsujimoto, T. (1995). Estimates for the pool size of releasable quanta at a single central synapse and for the time required to refill the pool. *Proc. Natl. Acad. Sci. U S A* 92, 846–849. doi: 10.1073/pnas.92.3.846

Stevens, C. F., and Wesseling, J. F. (1998). Activity-dependent modulation of the rate at which synaptic vesicles become available to undergo exocytosis. *Neuron* 21, 415–424. doi: 10.1016/s0896-6273(00)80550-4

Stölting, G., de Oliveira, R. C., Guzman, R. E., Miranda-Laferte, E., Conrad, R., Jordan, N., et al. (2015). Direct interaction of $Ca_V\beta$ with actin up-regulates L-type calcium currents in HL-1 cardiomyocytes. *J. Biol. Chem.* 290, 4561–4572. doi: 10.1074/jbc.M114.573956

Tadmouri, A., Kiyonaka, S., Barbado, M., Rousset, M., Fablet, K., Sawamura, S., et al. (2012). Cacnb4 directly couples electrical activity to gene expression, a process defective in juvenile epilepsy. *EMBO J.* 31, 3730–3744. doi: 10.1038/emboj.2012.226

Takamori, S., Holt, M., Stenius, K., Lemke, E. A., Grønborg, M., Riedel, D., et al. (2006). Molecular anatomy of a trafficking organelle. *Cell* 127, 831–846. doi: 10.1016/j.cell.2006.10.030

Tanifuji, S., Funakoshi-Tago, M., Ueda, F., Kasahara, T., and Mochida, S. (2013). Dynamin isoforms decode action potential firing for synaptic vesicle recycling. *J. Biol. Chem.* 288, 19050–19059. doi: 10.1074/jbc.m112.445874

Taschenberger, H., Woehler, A., and Neher, E. (2016). Superpriming of synaptic vesicles as a common basis for intersynapse variability and modulation of synaptic strength. *Proc. Natl. Acad. Sci. U S A* 113, E4548–E4557. doi: 10.1073/pnas.1606383113

Truckenbrodt, S., and Rizzoli, S. O. (2014). Spontaneous vesicle recycling in the synaptic bouton. *Front. Cell. Neurosci.* 8:409. doi: 10.3389/fncel.2014.00409

Van Petegem, F., Clark, K. A., Chatelain, F. C., and Minor, D. L. Jr. (2004). Structure of a complex between a voltage-gated calcium channel β-subunit and an α-subunit domain. *Nature* 429, 671–675. doi: 10.1038/nature02588

Vendel, A. C., Terry, M. D., Striegel, A. R., Iverson, N. M., Leuranguer, V., Rithner, C. D., et al. (2006). Alternative splicing of the voltage-gated Ca^{2+} channel β_4 subunit creates a uniquely folded N-terminal protein binding domain with cell-specific expression in the cerebellar cortex. *J. Neurosci.* 26, 2635–2644. doi: 10.1523/JNEUROSCI.0067-06.2006

Wang, S. S. H., Held, R. G., Wong, M. Y., Liu, C., Karakhanyan, A., and Kaeser, P. S. (2016). Fusion competent synaptic vesicles persist upon active zone disruption and loss of vesicle docking. *Neuron* 91, 777–791. doi: 10.1016/j.neuron.2016.07.005

Watanabe, S., Rost, B. R., Camacho-Perez, M., Davis, M. W., Sohl-Kielczynski, B., Rosenmund, C., et al. (2013). Ultrafast endocytosis at mouse hippocampal synapses. *Nature* 504, 242–247. doi: 10.1038/nature12809

Watanabe, S., Trimbuch, T., Camacho-Pérez, M., Rost, B. R., Brokowski, B., Sohl-Kielczynski, B., et al. (2014). Clathrin regenerates synaptic vesicles from endosomes. *Nature* 515, 228–233. doi: 10.1038/nature13846

Weiss, N. (2006). The calcium channel β_{4a} subunit: a scaffolding protein between voltage-gated calcium channel and presynaptic vesicle-release machinery? *J. Neurosci.* 26, 6117–6118. doi: 10.1523/JNEUROSCI.1699-06.2006

Wheeler, D. B., Randall, A., and Tsien, R. W. (1994). Roles of N-type and Q-type Ca^{2+} channels in supporting hippocampal synaptic transmission. *Science* 264, 107–111. doi: 10.1126/science.7832825

Williams, C. L., and Smith, S. M. (2018). Calcium dependence of spontaneous neurotransmitter release. *J. Neurosci. Res.* 96, 335–347. doi: 10.1002/jnr.24116

Wittemann, S., Mark, M. D., Rettig, J., and Herlitze, S. (2000). Synaptic localization and presynaptic function of calcium channel β_4-subunits in cultured hippocampal neurons. *J. Biol. Chem.* 275, 37807–37814. doi: 10.1074/jbc.m004653200

Wu, X. S., Lee, S. H., Sheng, J., Zhang, Z., Zhao, W. D., Wang, D., et al. (2016). Actin is crucial for all kinetically distinguishable forms of endocytosis at synapses. *Neuron* 92, 1020–1035. doi: 10.1016/j.neuron.2016.10.014

Wu, X. S., McNeil, B. D., Xu, J., Fan, J., Xue, L., Melicoff, E., et al. (2009). Ca^{2+} and calmodulin initiate all forms of endocytosis during depolarization at a nerve terminal. *Nat. Neurosci.* 12, 1003–1010. doi: 10.1038/nn.2355

Xie, M., Li, X., Han, J., Vogt, D. L., Wittemann, S., Mark, M. D., et al. (2007). Facilitation versus depression in cultured hippocampal neurons determined by targeting of Ca^{2+} channel $Ca_V\beta_4$ versus $Ca_V\beta_2$ subunits to synaptic terminals. *J. Cell. Biol.* 178, 489–502. doi: 10.1083/jcb.200702072

Yamashita, T. (2012). Ca^{2+}-dependent regulation of synaptic vesicle endocytosis. *Neurosci. Res.* 73, 1–7. doi: 10.1016/j.neures.2012.02.012

Conflict of Interest Statement: The authors declare that the research was conducted in the absence of any commercial or financial relationships that could be construed as a potential conflict of interest.